ACS Sustainable Chemistry & Engineering

Research Article

pubs.acs.org/journal/ascecg

Thermal Conversion of Lignin–Cellulose Composite Particles into Aggregates of Fine Carbon Grains Holding Micro- and Mesoporous Spaces

Takeshi Shimada,[†,‡] Toshimitsu Hata,[§] and Masashi Kijima*[,‡,⊥]

[†]Institute of Materials Science, Graduate School of Pure and Applied Sciences, University of Tsukuba, Tsukuba, Ibaraki 305-8573, Japan

[‡]Tsukuba Research Center for Interdisciplinary Materials Science, University of Tsukuba, Tsukuba, Ibaraki 305-8573, Japan

[§]Research Institute for Sustainable Humanosphere, Kyoto University, Gokasho, Uji, Kyoto 611-0011, Japan

[⊥]Division of Materials Science, Faculty of Pure and Applied Sciences, University of Tsukuba, Tsukuba, Ibaraki 305-8573, Japan

Supporting Information

ABSTRACT: Composite particles of lignin–hydroxyethylcellulose were fabricated by means of reverse-micelle formation using H_2O–$CHCl_3$ in the presence of a surfactant, and an aggregate of the particles was obtained by successive precipitation from acetone, filtration, and drying. The aggregate was carbonized by pyrolysis with heating up to 900 °C under flowing of argon. The carbonized product was a hierarchical porous carbon that had a Brunauer–Emmett–Teller (BET) surface area of 405 m^2/g with micropore volume (0.11 cm^3/g) and no small mesopore volume (0.58 cm^3/g). Higher-porous spherical-carbon aggregates were obtained by fitting an in situ surface activation in the carbon conversion process, i.e., composite particles similarly prepared from lignin and hydroxyethylcellulose in the presence of NaOH were carbonized. One of them showed a BET surface area of 1790 m^2/g with a micropore volume (0.54 cm^3/g) and large mesopore volume (2.08 cm^3/g). This in situ activation process added micropores and mesoporous cavities to the microporous carbon grains and enhanced development of mesoporous voids between the grains. The aggregate of the activated carbon grains in 1 M H_2SO_4 showed a good electrical double layer capacitance of 394 F/g at a current density of 0.05 A/g, which declined logarithmic functionally to 269 F/g at a higher current density of 0.4 A/g.

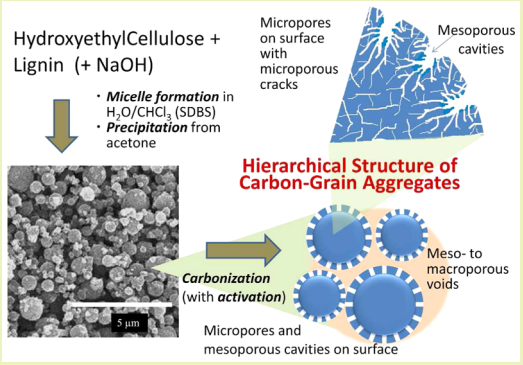

KEYWORDS: *Cellulose, Lignin, Porous carbon, Carbonization, Activation*

INTRODUCTION

Efficient thermal conversions of biomass resources that are produced by photosynthesis into valuable carbon-rich materials could be a consistent strategy to get the carbon cycle on earth back to normalcy and to sustain global environmental accumulation of carbon sources in living areas against excessive scattering of carbon sources into the atmosphere by huge consumption of fossil fuels since the last century. In recent years, porous carbons have been paid much attention as high performance materials for efficient energy use[1−3] and have been practically used in electric double layer capacitors, fuel cells, lithium ion batteries, hydrogen storage, and so on.[4−6] Therefore, development of functional porous carbon materials derived from biomass resources and wastes could be of benefit to mankind from the viewpoint of effective utilization of resources and energy. Various industrial functional carbon materials such as charcoal, activated carbons, and carbon blacks, have been directly manufactured from organized biomass by carbonization via top-down approach, but construction of highly functionalized carbon materials from each component of biomass by bottom-up approach is still primitive.

Lignin counteracted with alkaline (LA) is known as a waste material and a refined industrial extract of wood resources. Recently, high-porous carbons have been successfully prepared from LA and its structured derivatives by pyrolysis under flowing of argon without any additional activation processes.[7] The simple pyrolysis methods for the production of high-porous carbon[8,9] have been less investigated compared to the methods for the preparation of activated carbons.[10−12] Nano-to-micro structurations of starting substances as fine particle aggregates using a sol–gel process have been an effective way to bring meso- to macroporosity on nonporous polymer solids and their carbonized materials, as in a series of studies on carbon gels.[13−15] Therefore, addition of meso- to macroporosity to the microporous carbonized lignin has been

Received: November 19, 2014
Revised: June 11, 2015
Published: June 17, 2015

DOI: 10.1021/acssuschemeng.5b00230
ACS Sustainable Chem. Eng. 2015, 3, 1690−1695

Table 1. Preparation Conditions of LCC

sample	HEC (mg)	LA (mg)	NaOH (mg)	SDBS (mg)	H_2O (mL)	$CHCl_3$ (mL)	temperature[a] (°C)
LCC	100	200		400	6	30	r.t.
LCC1-a	100	200	300	1200	8	80	20
LCC2-a	100	200	300	900	4	60	20
LCC3-a	100	200	300	600	4	40	20

[a]Temperature for micelle formation.

attempted at the beginning.[7] The freeze-dried reverse micelle of LA did not give particle aggregates but instead fine-structured ones, whose carbonized materials had higher porosity with micro- to macropores than the carbons from nonstructured LA derivatives. As a result, high-porous carbons having S_{BET} values higher than 1400 m^2 g^{-1} with micro- to macropores were obtained by further structurations of LA and successive carbonization, although aggregates of uniform spherical carbons that have narrow distribution of mesopore widths like the carbon gels[13−15] were hard to be prepared. The low processability of LA and difficulty of keeping uniform particle shape are mainly due to the low molecular weight of LA.

On the other hand, cellulose is a high-molecular polysaccharide being used in various fields, and is the most abundant organic polymer on earth. There have been many reports on the carbonization of biological resources that contain cellulose, whereas reports on synthesis of carbon materials directly derived from cellulose are relatively few. Low carbonization yield and insolubility to solvents of cellulose might be reasons for lack of investigation. As far as recent studies on the preparation of functional carbon materials from cellulose, surface activations[16−18] have been key processes to add porosity to the carbonized materials. Hydrothermal treatments[19−21] also have been recognized to be remarkable processes to reconstitute cellulosic materials. Nevertheless, combination of lignin and cellulose is thought to be a best choice for production of nanostructured carbons from woody components among others, because the composite must have appropriate moldability and stiffness for nanostructuration and good thermal conversion yield to carbon. Practically, coelectrospinning of lignin and cellulose followed by carbonization could afford porous core−shell carbon fibers.[22]

In this study, spherical carbons are attempted to fabricate from LA and hydroxyethyl cellulose (HEC). The reason for using HEC is that it is a high-molecular cellulose derivative soluble in water and has high moldability, as it has been widely used as a thickener and binder in industries.[23] The combination of water-soluble LA and HEC enables us to make reverse micelles using heterogeneous mixed solvents of water and $CHCl_3$, and successive precipitation of the colloidal liquid from acetone can afford LA−HEC composite particles. The composite particles can be converted into aggregates of porous carbon grains by pyrolysis.

EXPERIMENTAL SECTION

Materials. Lignin counteracted with alkaline (LA) (trade name: alkaline lignin) was purchased from Tokyo Kasei Co. Ltd. As described in a previous report,[7] LA was soluble in water (pH = 8.81 at 0 °C), and the molecular weight was estimated to be about 350 g mol^{-1} by the freezing-point lowering method using a cryoscopic constant of H_2O (K_b = 1.86 K kg mol^{-1}). Hydroxyethyl cellulose (HEC) was purchased from Nacalai Tesque. Co. Ltd. Other chemicals used in this work were of reagent grade.

Preparation of Composite Particles of LA and HEC. LA (200 mg) and HEC (100 mg) in an H_2O (6 mL)−chloroform (30 mL) inhomogeneous medium in the presence of sodium dodecylbenzenesulfonate (SDBS) (400 mg) were mixed under an ultrasonic irradiation and vigorous stirring at room temperature. After the emulsification, the emulsion was dropped into a large amount of acetone with stirring to give a fine precipitation. The solid products were collected by filtration, washed well with acetone, and dried at 80 °C under vacuum for 3 h, giving lignin−cellulose composite particles (LCC), quantitatively. Similarly, LA (200 mg), HEC (100 mg), and NaOH (300 mg) composite particles (LCC1-a, LCC2-a, and LCC3-a) were prepared from reverse micelle of LA, HEC, and NaOH in the heterogeneous two-phase aqueous medium (H_2O:$CHCl_3$(mL) = 8:80, 4:60, and 4:40) in the presence of SDBS (1200, 900, and 600 mg) at 20 °C, followed by the precipitation from acetone, respectively. These reaction conditions are summarized in Table 1.

Carbonization. A fine powder of LA, HEC, LCC, and LCC-a (ca. 200 mg) on an alumina boat covered with an alumina plate was heated in a furnace (EKRO-12K, Isuzu) from room temperature to 900 °C at heating rate of 1 °C/min except the case for HEC (by heating at a rate of 10 °C/min from room temperature to 200 °C, 1 °C/min from 200 to 400 °C, and 10 °C/min from 400 to 900 °C) under flowing of argon. After the heating, the carbonized samples were cooled to room temperature under an argon atmosphere. Carbonization yields at 900 °C of these samples were comparable to or higher than those obtained from TG/DTA. The names of the samples were abbreviated as C-sample name, and the sample washed with distilled water was abbreviated as C-sample name-w. The carbonization yields of LCC-aw were given by (weight of C-LCC-aw at 900 °C)/(total weight of LA and HEC in LCC-a).

Measurements and Analyses. The thermogravimetry and differential thermal analysis (TG/DTA) of LA, HEC and LCC were carried out by an Extra 6000 TG/DTA (Seiko) under flowing of argon. The scanning electron microscope (SEM) images were acquired with a JSM-5510SEM (Jeol). The particle size distribution and average particle diameter of the samples (in $CHCl_3$) were measured by dynamic light scattering (DLS) with a DLS-6500 (Otsuka Electronics).

The pore structure of the samples was characterized with the N_2 adsorption isotherm at 77 K measured with a SA3100 (Coulter) and a Belsorp max (MicrotracBEL). Brunauer−Emmett−Teller (BET) specific surface area (S_{BET}) was obtained by the BET method.

The value of adsorbed volume at relative pressure (P/P_0) of 0.98 was adopted as total pore volume (V_{total}). According to the previous report,[7] the pore characterizations of the carbonized materials were also carried out by the α_s-plots for micropores and the Dollimore−Heal (DH) method for mesopores, respectively.[24,25] The subtracting pore effect (SPE) analysis of the α_s plots was also carried out to determine the total surface area (S_{total}), external surface area (S_{ext}), total micropore volume (V_{micro}), mesopore volume (V_{meso}), and average pore width (w_α) of micropores.[26]

The electrical double layer capacitances (EDLC) were measured by a galvanostatic charge/discharge technique at various current densities using a Hokutodenko HA301 constructed with three electrodes, i.e., a carbon sample wedged between Pt meshes as the working, a Pt plate as the counter, and a saturated calomel electrode (SCE) as the reference, in 1 M (mol dm^{-3}) H_2SO_4 under N_2. The carbon samples in a form of a disk pellet were prepared from respective carbon powders by mixing well with polyvinylidene fluoride (10 wt %) as a binder under a pressure of 4 MPa. Capacitances were normalized by weight (g) and BET surface area (m^2), respectively.

DOI: 10.1021/acssuschemeng.5b00230
ACS Sustainable Chem. Eng. 2015, 3, 1690−1695

RESULTS AND DISCUSSION

Preparation of Lignin–Cellulose Composite Particles (LCC). Because LA and HEC are soluble in water, it is possible to form reverse micelle of LA and HEC in a heterogeneous H_2O–chloroform medium in the presence of sodium dodecylbenzenesulfonate (SDBS) as the surfactant. The precipitation of the emulsion from acetone, washing with acetone, and drying under vacuum quantitatively afforded lignin–cellulose composite particles (LCC) as a fine powdery solid. The precipitation and washing processes are important to solidify the LA–HEC composites as grains and remove the surfactant. X-ray photoelectron spectroscopic (XPS) results and infrared absorption (IR) spectra suggest almost no presence of SDBS in LCC (Figures S1 and S2, Supporing information). The DLS analysis of LCC in $CHCl_3$ suggested that the average grain diameter was 790 ± 207 nm.

Thermal Analyses of LA, HEC, LCC and Properties of Their Carbonized Samples. Thermal behaviors of LA, HEC, and LCC in a form of powder were investigated by TG/DTA (Figure 1). The TG curve of LA indicates that the mass losses

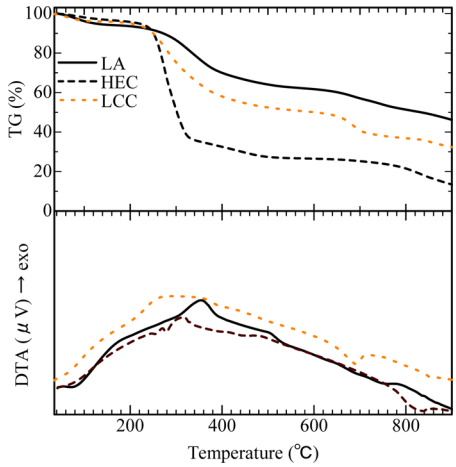

Figure 1. TG/DTA curves of LA, HEC, and LCC measured at a heating rate of 10 °C min^{-1} under flowing of argon.

were about 40% at 600 °C and 55% at 900 °C, which means that the carbonization yield of LA (45% at 900 °C) is higher compared to other woody materials.[16] By contrast, HEC shows low carbonization yield, i.e., the large mass losses about 75% at 600 °C and about 85% at 900 °C in the TG curve. LCC shows almost intermediate TG behavior between LA and HEC. On the other hand, the DTA curves did not show any apparent endothermal and exothermal peaks in the temperature range of 200–400 °C, although significant large mass-loss occurs around the temperature range in all cases. These results suggest that complex reactions involving eliminations and recombinations occur during the mass loss, and the exothermal reactions including recombination and cross-linking hidden in the thermograms could be a key process to produce thermostable carbon precursors in high yields.

On the basis of TG/DTA investigations, LA, HEC, and LCC samples were carbonized under various conditions to obtain porous carbons, and surface analysis of the carbonized materials (C-LA, C-HEC, C-LCC) were carried out by the N_2 adsorption–desorption analysis. The typical N_2 adsorption isotherms measured at 77 K are shown in Figure 2 and the results are summarized in Table 2.

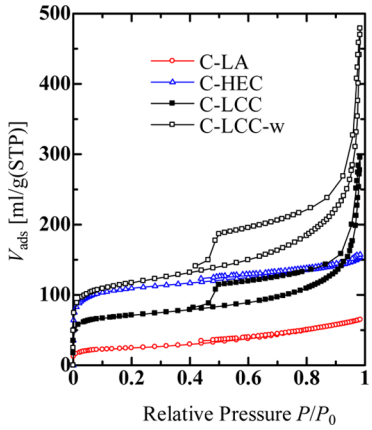

Figure 2. N_2 adsorption–desorption isotherms of C-LA, C-HEC, C-LCC, and C-LCC-w at 77 K.

The shapes of isotherms of C-LA and C-HEC are of type I according to classification of IUPAC,[24] which suggests that C-LA and C-HEC are microporous materials. The S_{BET} of C-LA was rather lower than the previous result,[7] which might be delicately affected by conditions for production of C-LA. The isotherms of C-LCC and its water-washed sample (C-LCC-w) showed a distinct hysteresis like the type IV with features of type I and type II, which suggests presence of mesopores in addition to micropores. They also characterized by the steep increase of amount of adsorption in the region of high relative pressure, which implies that they have considerable spaces of meso- to macropores. Moreover, washing of C-LCC with distilled water is effective to eliminate deposited inorganic salts derived from LA on the surface, giving C-LCC-w having higher S_{BET} and V_{total} values than those of C-LCC. If the material is an aggregate of fine particles that have a uniform size, the space between the particles is expected to be recognized as mesopores with a narrow distribution of the pore sizes.[14,24,27] C-LCC and C-LCC-w are attained to have the relatively large total pore volume (V_{total}), probably due to the material form of the carbon grain aggregates. Analysis of the N_2 adsorption isotherms by the DH method[25] showed that both have a broad distribution of mesopores whose pore widths are larger than 30 nm (Figure S3, Supporting Information).

Surface morphologies of LA, C-LA, HEC, C-HEC, LCC, C-LCC, and C-LCC-w are investigated by SEM and compared each other. Various shapes and sizes in several tens micro orders of smooth globular lumps of LA and fibrillar lumps of HEC were carbonized with retaining their morphologies (Figure S4, Supporting Information). In contrast to these uneven samples as received, LCC has a morphology of an aggregate of particles in various sizes of several hundred nanometers (Figure 3a). Particle sizes of LCC observed by SEM seem to be about within 500 nm, which is smaller than the average grain diameter of 790 nm determined by DLS. The difference might be due to different measuring conditions of the powdery samples between dried under vacuum and suspended in $CHCl_3$. After carbonization of LCC and successive washing with water, the surface morphology of C-LCC-w was similar to that of LCC (Figure 3b).

Properties of C-LCC-aw. To prepare carbon grain aggregates with higher specific surface areas than C-LCC, an in situ activation process is added into the preparation procedure for C-LCC. Reverse micelle of LA, HEC, and NaOH is possible to make in the H_2O–chloroform medium in

DOI: 10.1021/acssuschemeng.5b00230
ACS Sustainable Chem. Eng. 2015, 3, 1690–1695

Table 2. Carbonization Yields and Surface Analysis Results of Carbonized Samples

sample[a]	yield[b] (%)	S_{BET} (m^2/g)	S_{total} (m^2/g)	V_{micro} (mL/g)	w (nm)	V_{total} (mL/g)	V_{meso} (mL/g)
C-LA	39	86	94	0.014	0.71	0.099	0.085
C-HEC	14	379	441	0.13	0.75	0.24	0.11
C-LCC	36	245	300	0.068	0.67	0.42	0.35
C-LCC-w		405	479	0.11	0.71	0.69	0.58
C-LCC1-aw	18.1	1346	1430	0.35	0.83	2.59	2.24
C-LCC2-aw	21.1	1791	1973	0.54	0.79	2.62	2.08
C-LCC3-aw	17.6	1493	1626	0.48	0.81	1.68	1.20
AC[c]	1354	1550	0.49	0.77	0.84	0.35	

[a]C-LA, C-LCC, and C-LCC-a were prepared from LA, LCC, and LCC-a by heating at 1 °C/min from room temperature to 900 °C under flowing of Ar. C-HEC was prepared from HEC by heating at 10 °C/min from room temperature to 900 °C except 1 °C/min in the range of 200−400 °C under flowing of Ar. [b]Yield = (weight of C − X)/(total weights of LA and HEC in X) × 100 (%). [c]A commercial activated carbon.

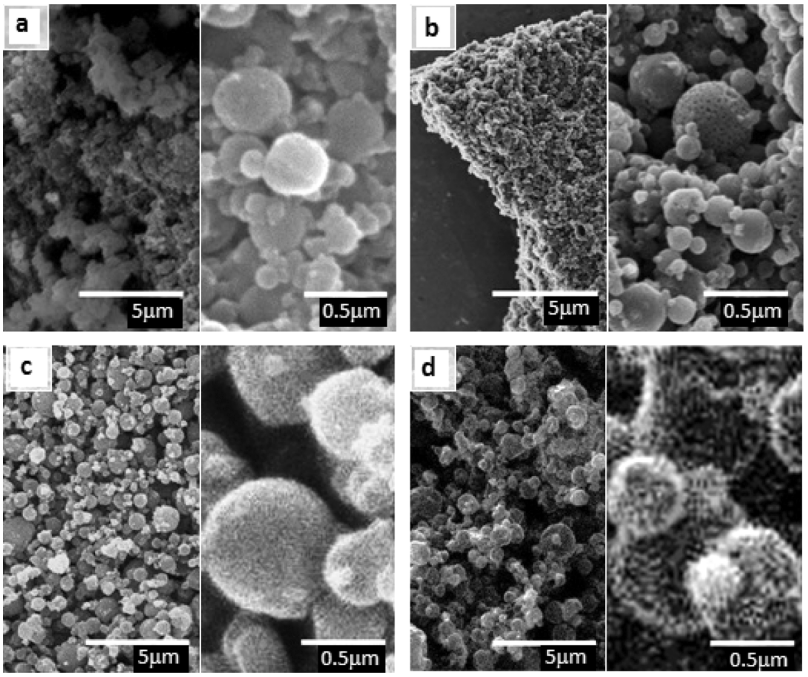

Figure 3. SEM images of (a) LCC, (b) C-LCC-w, (c) LCC2-a, and (d) C-LCC2-aw at magnifications of 5000× (left) and 40000× (right).

the presence of SDBS as the surfactant, because LA, HEC, and NaOH are well soluble in water. The micelles consisting of LA, HEC, and NaOH were prepared under various conditions described in the Experimental Section, and subsequent precipitation of the emulsion from acetone successfully gave composite particles (LCC1-a, LCC2-a, and LCC3-a), quantitatively. Successively, each LCC-a was carbonized by the steady heating up from room temperature to 900 °C at a rate of 1 °C/min. The carbonized samples were washing with water and dried, giving respective C-LCC-aw in about 20% yields.

The SEM images of LCC2-a shown in Figure 3c indicate an aggregate of composite particles similar to that of LCC (Figure 3a), whereas sizes of the particles are different. The difference of the particle size might be largely dependent on the preparation conditions. The average particle sizes of LCC1-a and LCC2-a were 671 ± 113 nm and 404 ± 39 nm, respectively, determined by DLS. The average grain size of LCC3-a could not be determined by DLS for the reason for polydispersity but the particle size was the largest among three in the sight of SEM observations. Carbonization of LCC-a and successive washing with water gave C-LCC-aw, which had almost the same shape and size as those of C-LCC-a but considerable rougher surface morphology as shown in Figure 3c,d.

The typical N_2 adsorption−desorption isotherms of C-LCC-aw and a reference sample of activated carbon (AC) are shown in Figure 4, and the surface analysis results of them are

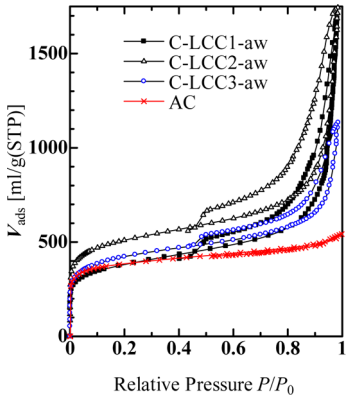

Figure 4. N_2 adsorption−desorption isotherms of C-LCC1-aw, C-LCC2-aw, C-LCC3-aw, and AC at 77 K.

DOI: 10.1021/acssuschemeng.5b00230
ACS Sustainable Chem. Eng. 2015, 3, 1690−1695

summarized in Table 1 together with the surface analysis results of carbonized LA, HEC, and LCC. The shapes of the isotherms of three C-LCC-aw showed a distinct hysteresis-like type IV in addition to type I and II features, which suggests presence of mesopores. DH analysis of C-LCC-aw shows that many mesopores are distributed in the range about 10−50 nm pore widths, which is narrower than those of LCC-1 (Figure S4, Supporting Information). Moreover, C-LCC2-aw had higher S_{BET} and considerably larger V_{total} values than those of C-LCC-w and AC, which could be ascribed to the micro- to mesoporous spaces newly developed during the surface activation process. The surface activation of the composite particles blended well with LA, HEC, and NaOH effectively, proceeded along with developing microporous spaces by the pyrolytic carbonization, which resulted in formations of micropores by pyrolysis and activation, development of mesoporous cavities by erosion of the micropores, and increment of mesoporous voids by intimate packing of the activated carbon grains. These features suggest that a series of C-LCC-aw has a hierarchical porous structure consisting of micropores, mesoporous cavities, and meso- to macroporous voids.

Lastly, electrical double layer capacitances (EDLC) of C-LCC-aw were measured in 1 M H_2SO_4 with a three-electrode system to confirm electrical function of the porous carbons, and the results are summarized in Figure 5a. C-LCC2-aw shows

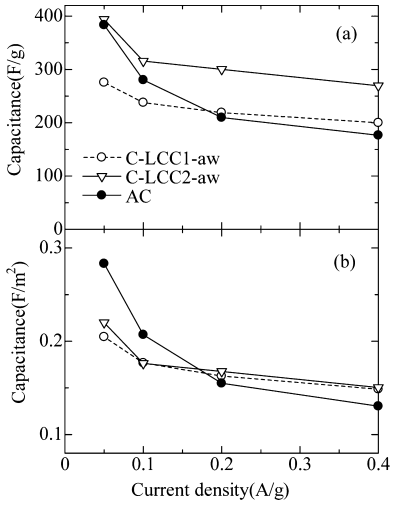

Figure 5. EDLC capacitances of C-LCC1-aw, C-LCC2-aw, and AC in 1 M H_2SO_4.

practically high gravimetric specific capacitance (C_g = 394 F/g) at a low current density (0.05 A/g). The commercial AC also showed a comparable value (C_g = 384 F/g) to that of C-LCC2-aw at 0.05 A/g. At the higher constant current density of 0.4 A/g, C_g of C-LCC2-aw declined logarithmic functionally to 269 F/g, whereas C_g of AC declined steeply to 177 F/g. The different behavior of decline of C_g between C-LCC-aw and AC is attributed to difference of porosity, i.e., the former is the hierarchical porous carbon-grain aggregate with micropores and mesoporous spaces and the latter is typical of a microporous carbon. The sufficient large mesopore volume for C-LCC-aw contributes to fast migration and diffusion of ions in the electrical double layers on the carbon surface, which is responsible for keeping the larger EDLC capacitances than those for AC in the faster discharge processes. Figure 5b shows the damping effect of capacitances per S_{BET} (C_s) against increase of current density. Accordance of C_s between C-LCC1-aw and C-LCC2-aw suggests that both carbons have similar hierarchical porous structures with similar surface activities on capacitance, although their surface areas are different.

It is obvious that C-LCC-aw has high EDLC performance in comparison with normal activated carbons prepared from biomass precursors reported previously; nevertheless, it is difficult to compare the EDLC performance measured under various conditions. In the results of EDLC measurements in 0.1 M H_2SO_4 equal to this experiment, a microporous carbon (S_{BET} = 1788 m^2/g) from sugarcane bagasse with $ZnCl_2$ activation showed a capacitance close to 300 F/g at 0.025 A/g,[28] whereas an N-containing (1.5 at. % by XPS) activated carbon (S_{BET} = 1019 m^2/g) from waste coffee grounds showed the higher capacitance, 368 F/g at 0.05 A/g.[29] Also, an activated carbon with N-content of 2 wt % (by XPS) and S_{BET} = 2062 m^2/g showed a high capacitance, 355 F/g at 0.125 A/g.[30] These higher values are due to the synergistic N-containing effects.[31,32] Under other conditions, activated carbons having S_{BET} about 1000−3000 m^2/g prepared from various biomass precursors by several activation methods showed capacitances about 100−350 F/g in aqueous electrolytic solutions.[33−35] It is generally recognized that (i) carbons having higher surface area show higher capacitance, (ii) presence of N on the carbon surface enhances capacitance characteristics in aqueous solution, and (iii) presence of sufficient mesoporous spaces stabilizes charge−discharge behavior for the reason for keeping moderate mobility of ions in the EDLC cell. It is noteworthy that C-LCC-aw that has the high S_{BET} = 1791 m^2/g with microporous and mesoporous surfaces on the carbon grains and meso- to macroporous interspaces of their aggregates resulted in substantially high capacitances despite the absence of N on the carbon surface.

CONCLUSIONS

The spherical composites of LA−HEC and LA−HEC−NaOH were prepared by the reverse-micelle formation and successive precipitation, which could be effectively converted to porous carbons up to 900 °C under an argon atmosphere, subsequent washing with water, and vacuum drying. They were fine spherical carbon aggregates, which had a hierarchical structure consisting of micropores and mesoporous cavities on the surface of each particle and meso- to macroporous spaces between the particles. The in situ activation of LCC-a during the carbonization was effective to obtain high porous carbons with large mesopore volume, which was applicable to EDLC.

ASSOCIATED CONTENT

Supporting Information

XPS spectra and elemental analysis data, IR spectra, mesopore distribution, SEM images of HEC, C-HEC, LA, and C-LA. The Supporting Information is available free of charge on the ACS Publications website at DOI: 10.1021/acssuschemeng.5b00230.

AUTHOR INFORMATION

Corresponding Author

*Masashi Kijima. Fax: +81 29 8534490. Tel: +81 29 8535295. E-mail: kijima@ims.tsukuba.ac.jp.

Notes

The authors declare no competing financial interest.

DOI: 10.1021/acssuschemeng.5b00230
ACS Sustainable Chem. Eng. 2015, 3, 1690−1695

■ ACKNOWLEDGMENTS

The authors thank Nippon Sheet Glass Foundation for Material Science and Engineering, and JSPS KAKENHI Grant Number 26410212 for financial support. This work was facilitated by sharing and cooperative system of the Chemical Analysis Center, University of Tsukuba, and also by collaborative research of Wood Composites Hall and Analysis and Development System for Advanced Materials (ADAM) at Research Institute for Sustainable Humanosphere (RISH), Kyoto University, for thermal analysis, N_2 adsorption measurements, dynamic light scattering, SEM, TEM, Raman, and XPS measurements.

■ REFERENCES

(1) Pandolfo, A. G.; Hollenkamp, A. F. Carbon properties and their role in supercapacitors. *J. Power Soures* **2006**, *157*, 11−27.
(2) Hu, Y. S.; Adelhelm, P.; Smarsly, B. M.; Hore, S.; Antonietti, M.; Maier, J. Synthesis of hierarchically porous carbon monoliths with highly ordered microstructure and their application in rechargeable lithium batteries with high-rate capability. *Adv. Funct. Mater.* **2007**, *17*, 1873−1878.
(3) Panella, B.; Hirscer, M.; Roth, S. Hydrogen adsorption in different carbon nanostructures. *Carbon* **2005**, *43*, 2209−2214.
(4) Bhattacharjya, D.; Kim, M. S.; Bae, T. S.; Yu, J. S. High performance supercapacitor prepared from hollow mesoporous carbon capsules with hierarchical nanoarchitecture. *J. Power Sources* **2013**, *244*, 799−805.
(5) Yun, Y. S.; Jin, H. J. Electrochemical performance of heteroatom-enriched amorphous carbon with hierarchical porous structure as anode for lithium-ion batteries. *Mater. Lett.* **2013**, *108*, 311−315.
(6) Minoda, A.; Oshima, S.; Iki, H.; Akiba, E. Synthesis of KOH-activated porous carbon materials and study of hydrogen adsorption. *J. Alloys Compd.* **2013**, *580*, 5301−5304.
(7) Kijima, M.; Hirukawa, T.; Hanawa, F.; Hata, T. Thermal conversion of alkaline lignin and its structured derivatives to porous carbonized materials. *Bioresour. Technol.* **2011**, *102*, 6279−6285.
(8) Kijima, M.; Tanimoto, H.; Takakura, K.; Fujiya, D.; Ayuta, Y.; Matsuishi, K. Characterization of porous carbonaceous materials derived from poly(phenylenebutadiynylene)s. *Carbon* **2007**, *45*, 594−601.
(9) Kobayashi, N.; Kijima, M. Microporous materials derived from two- and threedimensional hyperbranched conjugated polymers by thermal elimination of substituents. *J. Mater. Chem.* **2007**, *17*, 4289−4296.
(10) Bedia, J.; Rodriguez-Mirasol, J.; Cordero, T. Water vapour adsorption on lignin based activated carbons. *J. Chem. Technol. Biotechnol.* **2007**, *82*, 548−557.
(11) Fierro, V.; Torné-Fernández, V.; Celzard, A. Methodical study of the chemical activation of Kraft lignin with KOH and NaOH. *Microporous Mesoporous Mater.* **2007**, *101*, 419−431.
(12) Mussatto, S. I.; Fernandes, M.; Rocha, G. J. M.; Orfao, J. J. M.; Teixeira, J. A.; Roberto, I. C. Production, characterization and application of activated carbon from brewer's spent grain lignin. *Bioresour. Technol.* **2010**, *101*, 2450−2457.
(13) Pekala, R. W. Organic aerogels from the polycondensation of resorcinol with formaldehyde. *J. Mater. Sci.* **1989**, *24*, 3221−3227.
(14) Yamamoto, T.; Sugimoto, T.; Suzuki, T.; Mukai, S. R.; Tamon, H. Preparation and characterization of carbon cryogel microspheres. *Carbon* **2002**, *40*, 1345−1351.
(15) Kraiwattanawong, K.; Sano, N.; Tamon, H. Carbon tunnels formed in carbon/carbon composite cryogels. *Microporous Mesoporous Mater.* **2012**, *153*, 47−54.
(16) Khezami, L.; Chetouani, A.; Taouk, B.; Capart, R. Production and characterisation of activated carbon from wood components in powder: Cellulose, lignin, xylan. *Power Technol.* **2005**, *157*, 48−56.
(17) Guilminot, E.; Fischer, F.; Chatenet, M.; Rigacci, A.; Berthon-Fabry, S.; Achard, P.; Chainet, E. Use of cellulose-based carbon aerogels as catalyst support for PEM fuel cell electrodes: Electrochemical characterization. *J. Power Sources* **2007**, *166*, 104−111.
(18) Sun, M.; Hong, L.; Tan, G. M. Mesoporous activated carbon structure originated from cross-linking hydroxyethyl cellulose precursor by carboxylic acids. *J. Phys. Chem. C* **2011**, *116*, 352−360.
(19) Sevilla, M.; Fuertes, A. B. The production of carbon materials by hydrothermal carbonization of cellulose. *Carbon* **2009**, *47*, 2281−2289.
(20) Lu, X.; Pellechia, P. J.; Flora, J. R. V.; Berge, N. D. Influence of reaction time and temperature on product formation and characteristics associated with the hydrothermal carbonization of cellulose. *Bioresour. Technol.* **2013**, *138*, 180−190.
(21) Kong, L.; Miao, P.; Qin, J. Characteristics and pyrolysis dynamic behaviors of hydrothermally treated microcrystalline cellulose. *J. Anal. Appl. Pyrolysis* **2013**, *100*, 67−76.
(22) Xu, X.; Zhou, J.; Lubineau, G.; Chen, Y.; Wu, X. F.; Piere, R. Porous core-shell carbon fibers derived from lignin and cellulose nanofibrils. *Mater. Lett.* **2013**, *109*, 175−178.
(23) Ahmadi, R.; Burns, A. J.; Bruijn, J. D. Chitosan-based hydrogels do not induce angiogenesis. *J. Tissue Eng. Regener. Med.* **2009**, *4*, 309−315.
(24) Gregg, S. J.; Sing, K. S. *Adsorption, Surface Area and Porosity*; Academic Press; London, 1982.
(25) Dollimore, D.; Heal, G. R. Pore-size distribution in typical adsorbent systems. *J. Colloid Interface Sci.* **1970**, *33*, 508−519.
(26) Kaneko, K.; Ishii, C.; Kanoh, H.; Hanzawa, Y.; Setoyama, N.; Suzuki, T. Characterization of porous carbons with high resolution α_s-analysis and low temperature magnetic susceptibility. *Adv. Colloid Interface Sci.* **1998**, *76*−*77*, 295−320.
(27) Kubo, S.; White, R. J.; Tauer, K.; Titirici, M. Flexible coral-like carbon nanoarchitectures via a dual block copolymer−latex templating approach. *Chem. Mater.* **2013**, *25*, 4781−4790.
(28) Rufford, T. E.; Hulicova-Jurcakova, D.; Khosla, K.; Zhu, Z.; Lu, G. Q. Microstructure and electrochemical double-layer capacitance of carbon electrodes prepared by zinc chloride activation of sugar cane bagasse. *J. Power Sources* **2010**, *195*, 912−918.
(29) Rufford, T. E.; Hulicova-Jurcakova, D.; Zhu, Z.; Lu, G. Q. Nanoporous carbon electrode from waste coffee beans for high performance supercapacitors. *Electrochem. Commun.* **2008**, *10*, 1594−1597.
(30) Elmouwahidi, A.; Zapata-Benabithe, Z.; Carrasco-Marin, F.; Moreno-Castilla, C. Activated carbons from KOH-activation of argan (*Argania spinosa*) seed shells as supercapacitor electrodes. *Bioresour. Technol.* **2012**, *111*, 185−190.
(31) Frackowiak, E. Carbon materials for supercapacitor application. *Phys. Chem. Chem. Phys.* **2007**, *9*, 1774−1785.
(32) Oda, T.; Yamazaki, T.; Tazaki, Y.; Nakamura, J. Efficient thermal conversion of poly(pyridinediylbutadiynylene)s to nitrogen-containing microporous carbon. *Chem. Lett.* **2006**, *35*, 844−845.
(33) Du, S.; Wang, L.; Fu, X.; Chen, M.; Wang, C. Hierarchical porous carbon microspheres derived from porous starch for use in high-rate electrochemical double-layer capacitors. *Bioresour. Technol.* **2013**, *139*, 409−406.
(34) He, X.; Ling, P.; Qiu, J.; Yu, M.; Zhang, X.; Yu, C.; Zheng, M. Efficient preparation of biomass-based mesoporous carbons for supercapacitors with both high energy density and high power density. *J. Power Sources* **2013**, *240*, 109−113.
(35) Du, X.; Zhao, W.; Wang, Y.; Wang, C.; Chen, M.; Qi, T.; Hua, C.; Mac, M. Preparation of activated carbon hollow fibers from ramie at low temperature for electric double-layer capacitor applications. *Bioresour. Technol.* **2013**, *149*, 31−37.

DOI: 10.1021/acssuschemeng.5b00230
ACS Sustainable Chem. Eng. 2015, 3, 1690−1695